Low-dark current 10 Gbit/s operation of InAs/InGaAs quantum dot p-i-n photodiode grown on on-axis (001) GaP/Si

D. Inoue, Y. Wan, D. Jung, J. Norman, C. Shang, N. Nishiyama, S. Arai, A. C. Gossard, and J. E. Bowers

Citation: Appl. Phys. Lett. **113**, 093506 (2018); doi: 10.1063/1.5041908
View online: https://doi.org/10.1063/1.5041908
View Table of Contents: http://aip.scitation.org/toc/apl/113/9
Published by the American Institute of Physics

Low-dark current 10 Gbit/s operation of InAs/InGaAs quantum dot p-i-n photodiode grown on on-axis (001) GaP/Si

D. Inoue,[1,2,a)] Y. Wan,[1,a),b)] D. Jung,[1] J. Norman,[3] C. Shang,[3] N. Nishiyama,[2] S. Arai,[2] A. C. Gossard,[1,3] and J. E. Bowers[1,3]
[1]*Institute for Energy Efficiency, University of California Santa Barbara, Santa Barbara, California 93106, USA*
[2]*Institute of Innovative Research, Tokyo Institute of Technology, Tokyo 152-8552, Japan*
[3]*Materials Department, University of California Santa Barbara, Santa Barbara, California 93106, USA*

(Received 28 May 2018; accepted 18 August 2018; published online 30 August 2018)

We demonstrate 10 Gbit/s operation of InAs/InGaAs quantum dot (QD) p-i-n photodiodes (PDs) grown on on-axis (001) GaP/Si substrates. A $3.0 \times 50\ \mu m^2$ QD PD shows a small dark current of 0.2 nA at a bias voltage of −3 V, which corresponds to a dark current density of 0.13 mA/cm^2. This low-dark current characteristic obtained from a narrow-stripe device indicates that sidewall and threading dislocations have small effects on the dark current. The 3 dB bandwidth was 5.5 GHz at a bias voltage of −5 V. Large signal measurement with non-return-to-zero signals shows 10 Gbit/s eye opening. *Published by AIP Publishing*. https://doi.org/10.1063/1.5041908

Integration of III–V semiconductors on Si has been recognized as a key technology for high-density and low-cost manufacturing of optical devices.[1] Wafer bonding technology has realized III–V/SOI hybrid optical devices.[2] Flip-chip integration offers III–V light sources for passive optical circuits, such as planar-lightwave-circuits (PLCs) or silicon photonics circuits.[3] However, they require accurate alignment and multiple chip manipulation. For mass-manufacturing of III–V on Si devices, a wafer level process integration scheme is desired. Direct epitaxial growth of III–V semiconductors on a Si substrate can mitigate the complexity of III–V integration on Si.[4] The wafer scale integration based on an epitaxial growth can remove manipulation of III–V chips. III–V epitaxial growth on Si has been investigated for a long time to overcome the large lattice mismatch between III–V and Si. In the early stage of III–V lasers grown on Si, the active regions were bulk or quantum wells.[5,6] However, the reliability and lasing performance significantly deteriorated from lasers grown on III–V substrates due to high-density threading dislocations. To suppress generation of antiphase domains (APDs) at the interface of III–V and Si, a 4°–6° offcut substrate has been widely used,.[7,8] However, it is preferred to use a CMOS compatible on-axis (001) substrate for future mass manufacturing of III–V optical devices on Si. 1.3 μm InAs quantum dot (QD) lasers grown on V-groove patterned Si[9–11] and grown on on-axis (001) GaP/Si[12,13] showed successful low-threshold continuous-wave (CW) operations. A remarkable reduction in threading dislocation density (TDD) resulted in highly reliable and further low threshold current operation.[14,15] Recently, direct modulation characteristics of QD lasers grown on on-axis (001) GaP/Si were reported.[16] For monolithic integration of QD-based photonic integrated circuits (PICs) on Si, photodiodes (PDs) are needed as well as lasers.[17] A QD PD on Si has been demonstrated on a V-grooved Si substrate.[18] A $20 \times 50\ \mu m^2$ device showed a dark current of 4.8 nA (a dark current density of 0.48 mA/cm^2) at a bias voltage of −3 V and a 3 dB bandwidth of 2.3 GHz. A large-signal measurement of QD PDs grown on Si has thus far not been demonstrated. In addition to that, there is still room for reducing a dark current density and improving the bandwidth.

In this paper, we demonstrate 10 Gbit/s non-return-to-zero (NRZ) signal detection by QD PDs grown on on-axis Si. A significant reduction in TDD from $7.0 \times 10^7\ cm^{-2}$ to $8.4 \times 10^6\ cm^{-2}$ was obtained by using GaP/Si substrates. The $3 \times 50\ \mu m^2$ device showed a low dark current of 0.2 nA at the bias voltage of −3 V, which corresponds to a dark current density of 0.13 mA/cm^{-2}. A 3 dB bandwidth of 5.5 GHz was obtained, thanks to a narrow mesa waveguide structure. A large signal measurement of the QD PD on Si was performed, and a 10 Gbit/s eye opening was confirmed.

Figure 1 shows the QD PD epitaxial structure grown on a Si substrate. A GaAs buffer layer and GaAs/InGaAs dislocation filters (DFLs) were grown on the GaP/Si substrate. An AlGaAs graded-index (GRIN) separate-confinement-hetero (SCH) layer, 5QD absorption layers, and a *p*-GRIN SCH layer were subsequently grown. The epitaxial layers above the GaP layer were grown by solid-source molecular beam epitaxy. The atomic force microscopy image of the QD layer with a dot density of $4.9 \times 10^{10}\ cm^{-2}$ is shown in the inset of Fig. 1. This epitaxial structure is the same as used in fabrication of QD lasers in previous work.[13] The substrate with epitaxial layers was processed into a waveguide detector structure. A rectangular shape mesa waveguide was formed by an inductively coupled plasma etching. The etched surface was covered with Al_2O_3 by atomic layer deposition (ALD) to suppress surface leakage current. The detailed fabrication after growth can be found in Ref. 18. Figure 2 shows a schematic of the device structure. The cleaved facet was formed for light input from a lensed fiber. There are no-optical coatings on the cleaved facet.

Figure 3 shows the static characteristics of the fabricated QD PDs. The current-voltage characteristics were evaluated without illumination. Figure 3(a) shows the I-V characteristics

[a)]D. Inoue and Y. Wan contributed equally to this work.
[b)]Electronic mail: yatingwan@ucsb.edu

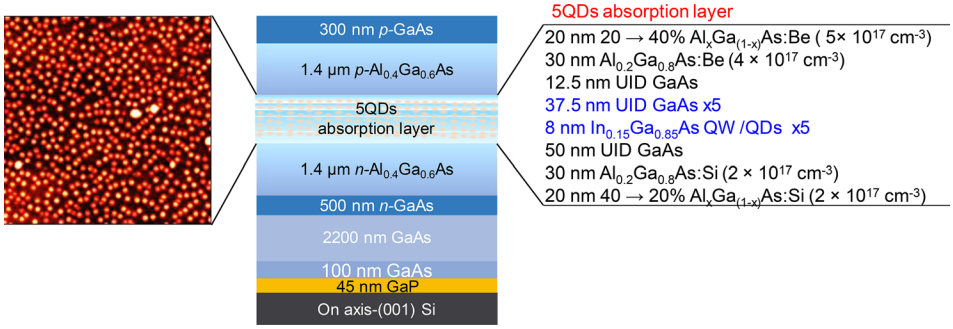

FIG. 1. Schematic of the epitaxial structure of 5QDs p-i-n PD grown on Si and AFM image of the QD layer.

of a $3 \times 50\ \mu m^2$ device. The dark current was 0.2 nA at the bias voltage of −3 V. The fluctuations in the measured current are attributed to the sensitivity limit of the instrument. The dark current density of 0.13 mA/cm^2 is less than 1/3 of our previous result (0.48 mA/cm^2 for a $20 \times 50\ \mu m^2$ device).[18] Although the QD PD in this work has a narrower stripe width than that of the previous work, no degradation in dark current density was observed. The reduction in dark current density is to the reduced TDD by optimizing the DFL and GaAs buffer.[19] The wavelength dependence of responsivity was evaluated for two devices with different device length. Figure 3(b) shows wavelength dependence of responsivity for 3×200 and $3 \times 50\ \mu m^2$ devices. The bias voltage was fixed at −1 V during the measurement for both devices. The coupling loss between a spherical-lensed fiber and the waveguide facet was assumed to be −3 dB. The Fabry-Perot resonance between the rear and front facets is due to the ∼30% reflection at the waveguide facets. The free spectral ranges (FSRs) of 5 nm and 11 nm correspond to their device lengths, respectively. Antireflection coating and a tilted facet would remove resonant behavior superimposed on their responsivity. By considering fiber coupling loss and facet reflection, the internal responsivities were 0.51 and 0.23 A/W for 200 μm and 50 μm devices, respectively. The QD layers have a ground state photoluminescence (PL) peak near 1280 nm. Absorption from the excited states is rather small compared with absorption from the ground state in this measurement wavelength range, since the energy level of the 1st excited state corresponds to an emission wavelength of 1180 nm.[13] Introduction of a resonant-cavity-enhanced structure with distributed-Bragg mirrors can improve the responsivity of QD PDs.[20] The responsivity of the 50-μm-long device was measured for various bias voltage conditions ranging from 0 to −9 V. Figure 3(c) shows wavelength dependence of responsivity measured

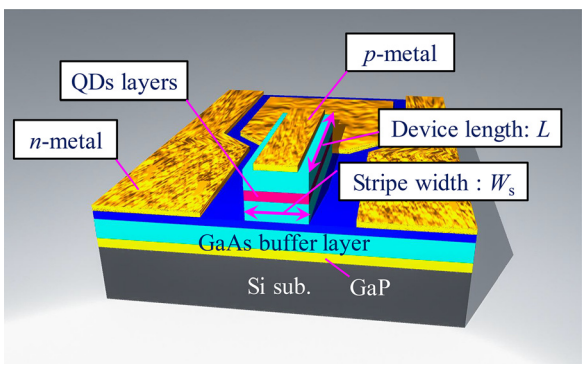

FIG. 2. Schematic image of the waveguide type QD PD grown on Si.

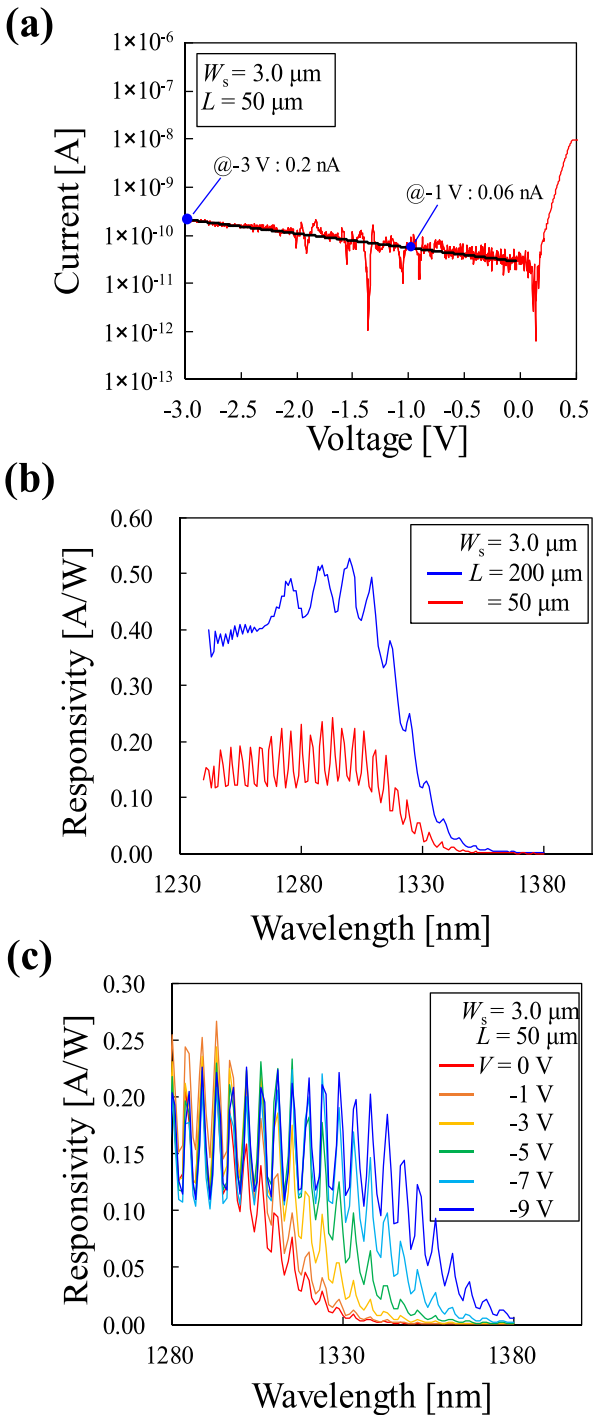

FIG. 3. Static characteristics of QD PD. (a) Current-voltage characteristics of the $3.0 \times 50\ \mu m^2$ device. (b) Wavelength dependence of responsivity for the devices with different lengths. (c) Wavelength dependence of responsivity measured with various bias voltage conditions.

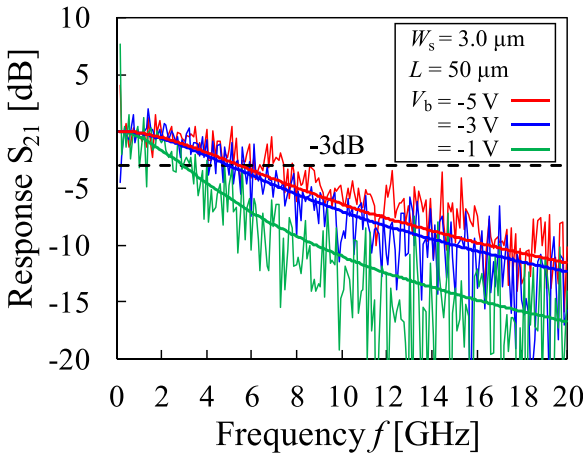

FIG. 4. Small-signal frequency responses of the $3.0 \times 50\ \mu m^2$ device for various bias voltages.

with various bias voltage conditions. As the reverse bias voltage was increased, the responsivity is extended toward longer wavelengths. This red shift was caused by the quantum-confined-stark-effect (QCSE) occurring in the QD absorption layer. By adjusting the absorption spectrum of the QD layer, O-band (1260–1360 nm) optical detection could be possible.

Next, the high-speed performance of the QD PD was characterized. A small-signal frequency response S_{21} was measured using a lightwave-component analyzer (LCA). A 1300 nm external laser was used for the measurement. A modulated light from the LCA was input to the device through a spherical lensed fiber. The polarization of the input light was controlled to be TE light by a polarization controller. The output voltage of the QD PD was analyzed by the electrical port of the LCA. Figure 4 shows the S_{21} characteristics of the $3 \times 50\ \mu m^2$ device for various bias voltages. The maximum 3 dB bandwidth was 5.5 GHz at −5 V. The capacitance of the QD PD was extracted by fitting the real and imaginary parts of the S_{22} measured by LCA. An equivalent circuit model used for the fitting can be found in Ref. 18. The photodiode capacitance C_j was measured to be 471 fF, which is approximately half of the previous results. The RC-limited bandwidth is calculated to be 6.2 GHz, which can explain obtained the maximum bandwidth of 5.5 GHz. The 3 dB bandwidth obtained in this work was greater than twice obtained in the previous report (2.3 GHz at −1 V). The reduced junction area from 1000 μm^2 ($20 \times 50\ \mu m^2$) to 150 μm^2 ($3.0 \times 50\ \mu m^2$) helps the bandwidth increase. There is a concern that carrier trapping in QDs limits the operation bandwidth. Our previous work demonstrated that hole trapping has a significant impact on the bandwidth.[18] Thinner barrier layers can assist tunneling extraction from the trappings under reverse biased conditions.

Table I summarizes the performance comparison between high-speed p-i-n photodiodes with different platform or materials. The first row shows a commercially available 10 Gbit/s class top-illuminated p-i-n photodiode.[21] A Ge waveguide photodiode on Si has wide bandwidths, thanks to its small junction area.[22] However, the dark current characteristics suffered from large leakage current due to high dislocation density. III–V/Si hybrid photodiodes can utilize high-quality InGaAs bulk absorption layer on Si platform.[23] A good responsivity, dark current and bandwidth have been achieved. Direct growth of III–V on the Si technique can enable us to fabricate photodiodes on a large-scale Si wafer. However, bulk InGaAs photodiodes grown on Si showed large dark current density due to threading dislocations generated at the interface between Si and III–V layer.[24,25] QD PDs directly grown on Si are attractive because monolithic integration with lasers and amplifiers is possible. On the contrary, Ge PDs on-Si have higher responsivity than QD PDs and gives an obvious speed advantage due to reduced junction capacitance. However, Ge PDs are made on the Si photonics platform, where efficient laser sources still need to be integrated by either wafer bonding or chip mounting. A QD PD grown on Si has proven its advantage in dark current characteristics. A QD PD on a V-grooved Si substrate with a TDD of $7 \times 10^7\ cm^2$ has a small dark current density of 0.48 mA/cm^2. In this work, a QD PD was grown on the high-quality buffer layer with a TDD of $8.4 \times 10^6\ cm^{-2}$. Since there is a problem that the QD PD has a relatively small responsivity compared with bulk absorption PD, it is necessary to introduce a resonant cavity enhanced structure. Increasing the number of QD layers is a straightforward way to address the small optical overlap on absorption layers. It should be noted that degradation of PL intensity was observed for QDs with more than 5 dot layers due to strain accumulation. Therefore, the growth conditions and core structure should be optimized to increase the number of QD layers while maintaining the total core thickness to avoid carrier transit delay. In addition, there is still room to improve the dot density of the absorption layers. Higher density QDs could achieve a larger absorption coefficient. By optimizing the growth condition, it is possible to achieve a dot density up to $6.6 \times 10^{10}\ cm^{-2}$.[26]

The eye diagram of the QD PD was measured using NRZ signals. Electrical modulation signals were generated

TABLE I. Performance comparison among high-speed p-i-n photodiodes.

	Responsivity for 1300 nm band (A/W)	Dark current (nA)	Dark current density (mA/cm^2) [Bias voltage (V)]	3 dB bandwidth (GHz)	Junction area (μm^2)	References
InGaAs bulk on InP	0.80	0.5	0.05 (−5 V)	9.0	1017	21
Ge on Si	0.98	3.5	49 (−2 V)	>50	7.1	22
InGaAs bonded on Si	0.45	1.6	3.2 (−4 V)	33	50	23
Direct growth of InGaAs bulk on Si	0.57	200	64 (−1 V)	10	314	24
Direct growth of InGaAs bulk on Si	0.22	2500	625 (−1 V)	9	400	25
Direct growth of QDs on Si	0.33	4.8	0.48 (−3 V)	2.3	1000	16
Direct growth of QDs on Si	0.08	0.2	0.13 (−3 V)	5.5	150	This work

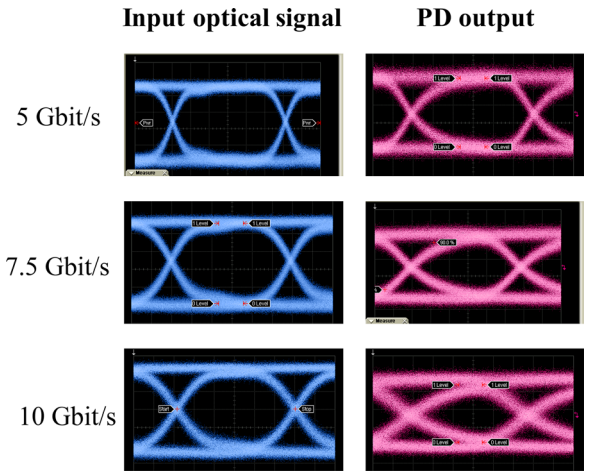

FIG. 5. Measured eye diagrams for data-rate ranging from 5 to 10 Gbit/s. The left column shows input optical signals. The right column shows PD output signals with a bias voltage of −5 V.

by a pulse pattern generator and applied to a lithium-niobate (LN) modulator. An intensity of an external tunable laser output was modulated by the LN modulator. The polarization of the modulated light was controlled to be TE light by a polarization controller. The modulated light signal was used as an input to the device through a spherical lensed fiber. The AC component of the PD output was separated by a bias-tee. Finally, the signals were captured and analyzed by a sampling oscilloscope. The modulation signal was NRZ with a pseudo-random-bit-sequence (PRBS) of 2^{31}-1. The device was biased at −5 V, which gave maximum 3 dB bandwidth. Figure 5 shows eye diagrams of the input optical signals generated by the LN modulator and output signals of the QD PD. The data-rates range from 5 to 10 Gbit/s. The average photocurrent under modulated optical input was approximately 0.12 mA. The clear eye opening up to a data-rate of 10 Gbit/s is consistent with the small-signal bandwidth of 5.5 GHz. The noise in the eye diagram mainly comes from the measurement instruments. The noise equivalent power of the QD PDs was not characterized at this time. The obtained results indicate that QD PDs can play an important role in QD-based monolithic PICs grown on the Si substrate.

In this paper, we have demonstrated 10 Gbit/s operation of 1.3 μm quantum dot photodiodes directly grown on on-axis (001) GaP/Si with low dark current. The reduced threading dislocation density enables us to realize a low-dark current density of 0.13 mA/cm^2 under −3 V bias condition. A 3 dB bandwidth of 5.5 GHz was obtained at a bias voltage of −5 V, which is twice as large as previous results. Large-signal characteristics of QD PDs were measured, and an eye opening up to 10 Gbit/s was confirmed with an NRZ optical signal input. We believe that these results will pave the way toward monolithic PICs directly grown on CMOS compatible Si substrates.

This research was supported by the Advanced Research Projects Agency-Energy (ARPA-E) DE-AR000067 and the Japan Society for the Promotion of Science (JSPS) Grants-in-Aid for Scientific Research (KAKENHI) (No. 15J11776). We are also grateful to Kurt Olsson and John English for their assistance in MBE maintenance and Di Liang, Chong Zhang, and Minh Tran for the fruitful discussions.

[1]J. E. Bowers, T. Komljenovic, M. Davenport, J. Hulme, A. Y. Liu, C. T. Santis, A. Spott, S. Srinivasan, E. J. Stanton, and C. Zhang, Proc. SPIE **9774**, 977402 (2016).
[2]A. W. Fang, H. Park, O. Cohen, R. Jones, M. J. Paniccia, and J. E. Bowers, Opt. Express **14**, 9203 (2006).
[3]S. Tanaka, S.-H. Jeong, S. Sekiguchi, T. Kurahashi, Y. Tanaka, and K. Morito, Opt. Express **20**, 28057 (2012).
[4]A. Y. Liu, S. Srinivasan, J. Norman, A. C. Gossard, and J. E. Bowers, Photonics Res. **3**, B1 (2015).
[5]T. H. Windhorn, G. M. Metze, B.-Y. Tsaur, and J. C. C. Fan, Appl. Phys. Lett. **45**, 309 (1984).
[6]M. Sugo, H. Mori, Y. Sakai, and Y. Itoh, Appl. Phys. Lett. **60**, 472 (1992).
[7]A. Y. Liu, C. Zhang, J. Norman, A. Snyder, D. Lubyshev, J. M. Fastenau, A. W. K. Liu, A. C. Gossard, and J. E. Bowers, Appl. Phys. Lett. **104**, 041104 (2014).
[8]S. M. Chen, W. Li, J. Wu, Q. Jiang, M. C. Tang, S. Shutts, S. N. Elliott, A. Sobiesierski, A. J. Seeds, I. Ross, P. M. Smowton, and H. Y. Liu, Nat. Photonics **10**, 307 (2016).
[9]J. Norman, M. J. Kennedy, J. Selvidge, Q. Li, Y. T. Wan, A. Y. Liu, P. G. Callahan, M. P. Echlin, T. M. Pollock, K. M. Lau, A. C. Gossard, and J. E. Bowers, Opt. Express **25**, 3927 (2017).
[10]Y. Wan, Q. Li, A. Y. Liu, A. C. Gossard, J. E. Bowers, E. L. Hu, and K. M. Lau, Opt. Lett. **41**, 1664 (2016).
[11]Y. Wan, J. Norman, Q. Li, M. J. Kennedy, D. Liang, C. Zhang, D. Huang, Z. Zhang, A. Y. Liu, A. Torres, D. Jung, A. C. Gossard, E. L. Hu, K. M. Lau, and J. E. Bowers, Optica **4**, 940 (2017).
[12]A. Y. Liu, J. Peters, X. Huang, D. Jung, J. Norman, M. L. Lee, A. C. Gossard, and J. E. Bowers, Opt. Lett. **42**, 338 (2017).
[13]D. Jung, J. Norman, M. Kennedy, C. Shang, B. Shin, Y. Wan, A. Gossard, and J. E. Bowers, Appl. Phys. Lett. **111**, 122107 (2017).
[14]D. Jung, P. Callahan, B. Shin, K. Mukherjee, A. Gossard, and J. E. Bowers, J. Appl. Phys. **122**, 225703 (2017).
[15]D. Jung, Z. Zhang, J. Norman, R. Herrick, M. Kennedy, P. Patel, K. Turnlund, C. Jan, Y. Wan, A. Gossard, and J. E. Bowers, ACS Photonics **5**, 1094 (2018).
[16]D. Inoue, D. Jung, J. Norman, Y. Wan, N. Nishiyama, S. Arai, A. C. Gossard, and J. E. Bowers, Opt. Express **26**, 7022 (2018).
[17]J. Norman, D. Jung, Y. Wan, and J. E. Bowers, APL Photonics **3**, 030901 (2018).
[18]Y. Wan, Z. Zhang, R. Chao, J. Norman, D. Jung, C. Shang, Q. Li, M. Kennedy, D. Liang, C. Zhang, J. Shi, A. C. Gossard, K. M. Lau, and J. E. Bowers, Opt. Express **25**, 27715 (2017).
[19]L. M. Giovane, H.-C. Luan, A. M. Agarwal, and L. C. Kimerling, Appl. Phys. Lett. **78**, 541 (2001).
[20]J. C. Campbell, D. L. Huffaker, H. Deng, and D. G. Deppe, Electron. Lett. **33**, 1337 (1997).
[21]See http://www.osioptoelectronics.com/Libraries/Datasheets/FCI-InGaAs-36C.sflb.ashx for performance of the InGaAs p-i-n photodiode (last accessed May 2, 2018).
[22]H. Chen, P. Verheyen, P. De Heyn, G. Lepage, J. De Coster, S. Balakrishnan, P. Absil, W. Yao, L. Shen, G. Roelkens, and J. Van Campenhout, Opt. Express **24**, 4622 (2016).
[23]R. A. Binetti, X. J. M. Leijtens, T. de Vries, Y. S. Oei, L. Di Cioccio, J. M. Fedeli, C. Lagahe, J. Van Campenhout, D. Van Thourhout, P. J. van Veldhoven, R. Notzel, and M. K. Smit, IEEE Photonics J. **2**, 299 (2010).
[24]Y. Gao, Z. Zhong, S. Feng, Y. Geng, H. Liang, A. W. Poon, and K. M. Lau, IEEE Photonics Technol. Lett. **24**, 237 (2012).
[25]S. Feng, Y. Geng, K. M. Lau, and A. W. Poon, Opt. Lett. **37**, 4035 (2012).
[26]T. Kageyama, Q. H. Vo, K. Watanabe, K. Takemasa, M. Sugawara, S. Iwamoto, and Y. Arakawa, in *Proceedings of the Compound Semiconductor Week 2016 (CSW'2016)*, Toyama, Japan (2016), p. MoC3-4.